⌘ *Author's Choice*

THE JOURNAL OF BIOLOGICAL CHEMISTRY VOL. 283, NO. 52, pp. 36280–36289, December 26, 2008

Caspase 8 Promotes Peripheral Localization and Activation of Rab5*[S]

Received for publication, July 31, 2008, and in revised form, September 25, 2008 Published, JBC Papers in Press, October 29, 2008, DOI 10.1074/jbc.M805878200

Vicente A. Torres[‡], Ainhoa Mielgo[‡], Daniela Barilà[§], Deborah H. Anderson[¶], and Dwayne Stupack[‡1]

From the [‡]Department of Pathology, University of California San Diego School of Medicine and the UCSD Moores Cancer Center, La Jolla California 92093, the [§]Department of Biology, University of Rome Tor Vergata and Laboratory of Cell Signaling, Istituto di Ricovero e, Cura a Carattere Scientifico Fondazione Santa Lucia, 00179, Rome, Italy, and the [¶]Cancer Research Unit, Saskatchewan Cancer Agency, Saskatoon, Saskatchewan, Canada S7N 4H4

Caspase 8 is a cysteine protease that initiates apoptotic signaling via the extrinsic pathway in a manner dependent upon association with early endosomes. Previously, we identified caspase 8 as an effector of migration, promoting motility in a manner dependent upon phosphorylation on Tyr-380 by Src family kinases and its subsequent association with Src homology 2 domain-containing proteins. Here we demonstrate the regulation of the small GTPase Rab5, which mediates early endosome formation, homotypic fusion, and maturation by caspase 8. Regulation requires the Tyr-380 phosphorylation site but not caspase proteolytic activity. Tyr-380 is essential for interaction with the Src homology 2 domains of p85α, a multifunctional adaptor for phosphatidylinositol 3-kinase, that possesses Rab-GAP activity. Interaction between caspase 8 and p85α promotes Rab5 GTP loading, alters endosomal trafficking, and results in the accumulation of Rab5-positive endosomes at the edge of the cell. Conversely, caspase 8-dependent GTP loading of Rab5 is overcome by increased expression of p85α in a Rab-GAP-dependent manner. Thus, we demonstrate a novel function for caspase 8 as a modulator of p85α Rab-GAP activity and endosomal trafficking.

Rab5 is a small GTPase involved in clathrin-coated vesicle formation, vesicle-early endosome, and early endosome homotypic fusion as well as endosome maturation (for review, see Refs. 1 and 2). Rab5 cycling between the GDP- (inactive) and GTP-bound (active) forms is a process tightly controlled by GTPase-activating proteins (GAPs),[2] guanine nucleotide-exchange factors, and GDP dissociation inhibitors. This strict control is critical to the correct "activation" of Rab5 in time and space (1).

GTP-bound Rab5 binds many effectors, including EEA1 (3), Rabaptin5 (4), Rabenosyn5 (5), and phosphatidylinositol 3-kinases (6), thus accounting for its influence on endosome tethering, fusion, and transport (2). The amount of GTP-loaded Rab5 acts as a rate-limiting step influencing the extent of endosome docking and fusion (7). Characterization of GAPs and guanine nucleotide-exchange factors continues to provide new insights on how membrane trafficking is regulated. Recently we characterized the p85α subunit of phosphatidylinositol 3-kinase as a Rab-GAP, binding Rab5 via its BH domain, providing a "timing" mechanism for GTP-bound Rab5 (8). Mutation in the BH domain (R274A) impairs Rab-GAP activity, altering the trafficking and degradation of tyrosine kinase receptors (9).

Caspase 8 is a cysteine protease that initiates apoptotic signaling via the extrinsic pathway in a manner dependent upon association with early endosomes (10–12). However, increasing evidence has revealed unexpected non-apoptotic functions of caspase 8, including enhancement of cell adhesion and motility (13–17). Importantly, after phosphorylation (13, 21) caspase 8 was shown to influence cell adhesion and migration via an interaction with p85α in a Rac-dependent manner (16).

Interestingly, Rab5 was recently shown to regulate cell motility, acting in concert with Rac activation at the leading edge of the cells (23, 24). As caspase 8 was previously shown to associate with peripheral endosomes, we speculated that caspase 8 might influence Rab function. Here we show that caspase 8 influences the organization of Rab5-containing early endosomes via association with, and sequestration of p85α. This promotes Rab5 GTP loading, inhibits endosomal maturation, and promotes accumulation of Rab5-positive endosomes at the edge of the cell. The caspase 8-dependent GTP loading of Rab5 can be overcome by increasing the expression of p85α but requires the phosphotyrosine binding activity of the SH2 domains as well as the Rab-GAP activity within the BH domain of p85α. Thus, we reveal a new function for caspase 8 as a regulator of p85α Rab-GAP activity and endosomal trafficking.

EXPERIMENTAL PROCEDURES

Materials—Polyclonal anti-caspase 8 (catalog #559932) and monoclonal anti-caspase 8 (catalog #551242) antibodies were from BD Pharmingen. Mouse monoclonal anti-Rab5 (catalog #sc46692), monoclonal anti-p85α (catalog #sc1637), and rabbit polyclonal anti-Rab7 (catalog #sc10767) antibodies were from

* This work was supported, in whole or in part, by National Institutes of Health Grant CA107263 (NCI, to D. S.). This work was also supported by Canadian Cancer Society, Saskatchewan Division Grant 019040 (to D. A.) and by grants from the Italian Association for Cancer Research and International Association for Cancer Research Grant AICR 07-0461 (to D. B.). The costs of publication of this article were defrayed in part by the payment of page charges. This article must therefore be hereby marked "*advertisement*" in accordance with 18 U.S.C. Section 1734 solely to indicate this fact.

⌘ *Author's Choice*—Final version full access.

[S] The on-line version of this article (available at http://www.jbc.org) contains supplemental Figs. 1–7.

[1] To whom correspondence should be addressed: Moores UCSD Cancer Center, 3855 Health Sciences Way, MC0803, La Jolla CA 92093-0803. Tel.: 858-822-1150; Fax: 858-822-2630; E-mail: dstupack@ucsd.edu.

[2] The abbreviations used are: GAP, GTPase-activating protein; BH, breakpoint cluster region homology domain; EEA1, early-endosomal autoantigen 1; GST, glutathione *S*-transferase; HRP, horseradish peroxidase; LDL, low density lipoprotein; M6PR, cation-independent mannose 6-phosphate receptor; SH2, Src homology 2; FL, full-length; PBS, phosphate-buffered saline; BSA, bovine serum albumin; GFP, green fluorescent protein.

Santa Cruz Biotechnology. Polyclonal anti-EEA1 (catalog #ab50313) and polyclonal anti-M6PR (catalog #ab32815) antibodies were from Abcam (Cambridge, MA). Goat anti-rabbit and goat anti-mouse antibodies coupled to horseradish peroxidase (HRP) and monoclonal anti-actin antibody (catalog #A5316) were from Bio-Rad. Alexa Fluor® 488- and Alexa Fluor® 555-labeled secondary antibodies, Alexa Fluor® 488-labeled transferrin (catalog #T13342), BODIPY® FL low density lipoprotein (LDL; catalog #L3483), and TO-PRO®-3 (catalog #T3605) were from Molecular Probes (Eugene, OR). The FuGENE 6 Transfection Reagent was from Roche Diagnostics. The PureLink™ Quick Plasmid Miniprep (catalog #K2100-10) and PureLink™ Hipure Plasmid Filter Purification (catalog #K2100-17) kits were from Invitrogen. Geneticin® (G418 sulfate, catalog #11811) was from Invitrogen. Cell medium and antibiotics were from Cellgro™ Mediatech, Inc (Herndon, VA). Fetal bovine serum (catalog #SH30070.03) was from HyClone (Logan, UT). Peroxidase from HRP and the peroxidase substrate 2,2′ azino-bis(3-ethylbenzthiazoline-6-sulfonic acid) (ABTS) were from Sigma. Glutathione-Sepharose™ 4B was from GE Healthcare. Chemiluminescent substrate (catalog #34078) and protein A/G beads were from Pierce. Protease inhibitors mixture tablets were from Roche Diagnostics.

Cell Culture—293T and A549 cells were cultured in Dulbecco's modified Eagle's medium supplemented with 10% fetal bovine serum and antibiotics (10,000 units/ml penicillin, 10 μg/ml streptomycin) at 37 °C, 5% CO_2. The previously described human neuroblastoma cells NB7 and NB7C8 were cultured in RPMI with 10% fetal bovine serum and antibiotics (20). Lentiviral-mediated down-regulation of caspase 8 in A549 cells by short hairpin RNA was previously described (25). Stably transfected cells were maintained in presence of 400 μg of puromycin. For transient transfection experiments in HEK293T, NB7, and NB7C8 cells, the reagent FuGENE® was used following the instructions provided by the manufacturer.

Plasmids—Rab5 mutants were described elsewhere (26). Wild type Rab5 and the mutants Rab5/S34N and Rab5/Q79L were subcloned from pET3C vector (a kind gift from Dr. S. Schmid, the Scripps Research Institute) into pcDNA3.1(+) by PCR using the primers 5′-cgggatccatggctaatcgaggagcaaca-3′ and 5′-cccgcggccgcttagttactacaacactgact-3′ and the restriction sites BamHI/NotI. The previously described "Rab5 binding domain" comprising the last 73 amino acids of Rabaptin-5 (residues 789–862) was obtained by PCR using human Rabaptin5 cloned into pCMV-SPORT6 (Invitrogen) as a template and the primers 5′-cccgcggccgctcatgtctcaggaagctggt-3′and 5′-cggtcgacaagctaaggctaccgttgaaca-3′. The PCR product was digested and ligated into pGEX-6P1 (GE Healthcare) by using the restriction sites SalI/NotI. Human caspase 8 was available in the pcDNA3.1(+) and pEGFP-N2 vectors, as previously described (13, 19). The caspase 8 mutants C360A and Y380F were previously reported and cloned into pEGFP-N2 vector (13). Bovine FLAG-tagged wild type p85α, p85α/R274A (mutant defective for Rab-GAP activity), and p85α/R368A/R649A (double mutant ΔR, defective in both SH2 domains via point mutations) were previously described (8).

Immunofluorescence—Cells were grown for 24 h on glass coverslips and subjected or not to treatment as indicated. After rinsing with PBS, cells were fixed in PBS, 4% paraformaldehyde (10 min), permeabilized with 0.1% Triton X-100 (5 min), and blocked with 2% BSA in PBS (30 min) at room temperature. Cells were then incubated with either monoclonal anti-Rab5 IgG (1:50), polyclonal anti-Rab7 IgG (1:50), polyclonal anti-M6PR IgG (1:50), or polyclonal anti-EEA1 (1:250) primary antibodies followed by incubation with the respective Alexa Fluor® conjugated secondary antibodies (1:250). Nuclei were stained with TO-PRO®-3 (1:500). Samples were then washed and mounted onto slides with the Vectashield Hard-Set mounting media (Vector Laboratories, Burlingame, VT) and visualized on a Nikon Eclipse C1 confocal microscope with a 1.4 NA 60× oil immersion lens using minimum pinhole (30 μm). Images were captured using EZ-C1 3.50 imaging software and analyzed using National Institutes of Health ImageJ software.

Image Analysis; Measurement of the Incidence of Cells with Peripheral Rab5—Pictures were randomly chosen, and cells were comparatively defined as "positive for periphery Rab5 staining" or "negative for periphery Rab5 staining" based on the high or low relative staining for Rab5 at cell periphery. Then the percentage of "positive cells" was calculated with respect to the total cell number. Total cell number was counted by nuclear staining (ToPRO3). For quantification of peripheral Rab5, pictures were randomly chosen, and round-shaped cells were picked for individual analysis. Cell periphery was defined as the area between the cell surface and 2–3 μm beneath (in cells ranging between 20 and 25 μm in diameter). This area corresponds to the ~25% outer layer of the cell. Relative levels of Rab5 were calculated within this area by using the "Radial Profile Plugin" of the ImageJ software. A total of six cells per picture, five pictures per experiment in a total of three independent experiments was analyzed. For analysis, the red channel (Rab5 staining) was adjusted to a window/level of 160 pixels, and then a radial profile was drawn around the cell (outer circle). The integrated density of pixels was measured within this outer circle. Thereafter, a second radial profile (inner circle) was drawn with a radius of 3/4 of the outer circle. The integrated density of pixels was measured within this inner circle. Finally, an arbitrary estimation of the percentage of peripheral Rab5 was calculated as % peripheral Rab5 = 100 − (no. of pixels inner circle/no. of pixels outer circle).

Co-localization Analysis—ImageJ software was used for analysis. First, both red and green channels to be analyzed were adjusted to a window/level of 160 pixels, and the integrated intensity of pixels for each channel was measured. Thereafter, the integrated intensity of pixels co-localized was measured by using the "Co-localization RGB Plugin" of ImageJ.

Immunoblotting—Cell extracts were prepared in radioimmune precipitation assay buffer (100 mM Tris base, 150 mM NaCl, 1 mM EDTA, 1% deoxycholic acid, 1% Triton X-100, 0.1% SDS, 50 mM NaF) containing protease inhibitors, boiled in Laemmli buffer, and separated by SDS-PAGE on 10 or 12% acrylamide minigels (Bio-Rad) by loading 25 μg of total protein per lane and transferred to nitrocellulose. Blots were blocked with 5% milk in 0.1% Tween, PBS and then probed with anti-actin (1:5000), anti-Rab5 (1:500), anti-Rab7 (1:300), anti-EEA1 (1:1000), or anti-M6PR (1:2500) antibodies. Bound antibodies

were detected with horseradish peroxidase-conjugated secondary antibodies and the ECL system.

Transient Transfections—Cells were grown for 24 h in complete medium at 50–70% confluence. Transfections were performed with 10 μg of the indicated plasmids by using the FuGENE® system according to the manufacturer's instructions. Post-transfection, extracts were obtained and subjected to either immunoprecipitation or pulldown analysis.

Immunoprecipitation—Cell extracts were prepared in a buffer containing 20 mM Tris, pH 7.4, 150 mM NaCl, 1% Nonidet P-40, and protease inhibitors. Supernatants obtained after centrifugation (13,000 $\times$ *g*, 5 min, 4 °C) were used for immunoprecipitation assays (500 μg of total protein per assay) with protein A/G beads-immobilized antibody. Caspase 8 was immunoprecipitated with mouse monoclonal anti-caspase 8. The immunoprecipitated samples were solubilized in Laemmli buffer, boiled, and separated by SDS-PAGE and analyzed by Western blotting as indicated above.

GTP-loaded Rab5 Pulldown Assay—The Rab5 pulldown assay was performed as previously described (27, 28) with some modifications. After treatment, cell extracts were prepared in lysis buffer containing 25 mM HEPES, pH 7.4, 100 mM NaCl, 5 mM $MgCl_2$, 1% Nonidet P-40, 10% glycerol, 1 mM dithiothreitol, and protease inhibitors. Extracts were incubated by 5 min on ice and clarified by centrifugation (10,000 $\times$ *g*, 1 min, 4 °C). Post-nuclear supernatants were used immediately for pulldown assays by adding 150 μg of precoated beads. GSH beads were precoated with 100 μg of GST-R5BD by 1 h at 4 °C. Pulldown incubations were carried out by 15 min in a rotating shaker at 4 °C. Thereafter, beads were collected and washed 3 times with lysis buffer containing 0.01% Nonidet P-40 and protease inhibitors. Samples were solubilized in Laemmli buffer, boiled, and separated by SDS-PAGE and analyzed by Western blotting as indicated above.

Endosome Fractionation in Sucrose Gradients—Endosome fractionation and HRP uptake assays were performed as previously described (29, 30). Briefly, cells were grown in 15-cm plates for 24 h in complete medium. Cell monolayers were washed in PBS and incubated at 37 °C with 5 ml of 2 mg/ml HRP in minimal essential medium supplemented with 10 mM glucose and 10 mM HEPES, pH 7.4 (internalization medium), at the indicated times. Incubations were stopped on ice by washing cells thoroughly with PBS at 4 °C. Cells were scraped, collected by centrifugation at 1500 rpm at 4 °C for 5 min in a Sorvall RT 6000D centrifuge. Cells were then washed with 10 ml of ice-cold PBS, centrifuged at 1700 rpm at 4 °C for 5 min and finally resuspended in homogenization buffer (250 mM sucrose, 1 mM EDTA, 3 mM imidazole, pH 7.4), centrifuged at 2000 rpm at 4 °C for 10 min. The cell pellet was resuspended in 500 μl of homogenization buffer containing protease inhibitors and homogenized by 8 passages through a 22½-gauge needle in a 1-ml syringe (BD Biosciences). Post-nuclear supernatants were obtained by centrifuging homogenates 10 min at 3000 rpm at 4 °C in a bench Eppendorf centrifuge. The post-nuclear supernatants (PNS) was brought to 40.6% sucrose by mixing 400 μl of PNS with 600 μl of 60% sucrose in homogenization buffer buffer. A gradient was prepared by overlaying 1 ml of homogenate, 40.6% sucrose, 2 ml of 35% sucrose, 1.5 ml of 30% sucrose, 400 μl homogenization buffer (8% sucrose) in a SW55Ti centrifuge tube. The gradient was centrifuged at 36,000 rpm (125,000 $\times$ *g*) for 66 min at 4 °C in a Beckman L7–65 ultracentrifuge. Endosome fractions were collected as follows; early endosomes at the 30/35% sucrose interface and late endosomes at the 8/30% sucrose interface. For protein screening, 45 μl of each fraction was mixed with sample buffer and loaded onto 10% acrylamide minigels. To measure the relative amount of endocytosed HRP and the distribution in endosome fractions, 2–10 μl of each fraction was incubated with 2,2′ azino-bis(3-ethylbenzthiazoline-6-sulfonic acid) (Sigma) and read at 405 nm according to the manufacturer's protocol.

LDL and Transferrin Internalization and Recycling Assays—NB7 and NB7C8 cells were grown at confluence in complete medium for 24 h. Thereafter, cells were detached with trypsin, centrifuged, re-suspended with 0.2% BSA in minimal essential medium supplemented with 10 mM glucose, 10 mM HEPES, pH 7.4 (internalization medium), and incubated for 30 min at 37 °C. For internalization experiments, 250 μl of aliquots of cell suspensions (5 $\times$ 10^5 cells) were placed in 1000-μl test tubes. Cells were centrifuged and resuspended with 0.2% BSA in internalization medium containing either 30 μg/μl Alexa Fluor® 488-labeled transferrin or 5 μg/μl BODIPY® FL LDL at 4 °C. Incubations were carried out at 37 °C and stopped on ice at different time points as indicated. Thereafter, cells were washed with ice-cold PBS, fixed with 0.5% paraformaldehyde, and resuspended with 2% BSA in PBS. For recycling experiments, cells were incubated with 30 μg/μl of Alexa Fluor® 488-labeled transferrin as indicated above for 15 min. Then samples were immediately placed in ice, washed with ice-cold PBS, re-suspended with 0.2% BSA in internalization medium, and incubated at different times at 37 °C. Cells were then collected, washed, and fixed as indicated above. Samples were analyzed by fluorescence-activated cell sorter (FACSCalibur) using the CellQuest Pro® software.

Statistical Analysis—Where pertinent, results were compared using unpaired *t* tests of at least three independent experiments or as indicated. A p value <0.05 was considered significant.

RESULTS

Caspase 8 Induces Accumulation of Rab5 Endosomes at Cell Periphery—Emerging evidence suggests that caspase 8 influences cellular adhesion and migration (22) likely via activation of Rac at the cell periphery (15, 16). Interestingly, Rac function is spatially regulated by the endocytic protein Rab5 during cell migration (23). To explore this potential link between caspase 8 and endocytic machinery, we first evaluated the cellular distribution of several endocytic markers in cells expressing or deficient for caspase 8. To this end we used the previously reported neuroblastoma cells NB7, which lack endogenous caspase 8 and those stably reconstituted for "physiological" levels of caspase 8 (*i.e.* higher expression than NB5 but lower than NB16) (19, 20). We assessed the distribution of early endosomal markers (EEA1 and Rab5) and late endosomal or lysosomal proteins (Rab7 and the cation-independent mannose-6 phosphate receptor (M6PR)) in this model. Interestingly, the localization of Rab5 differed in cells expressing caspase 8 relative to caspase

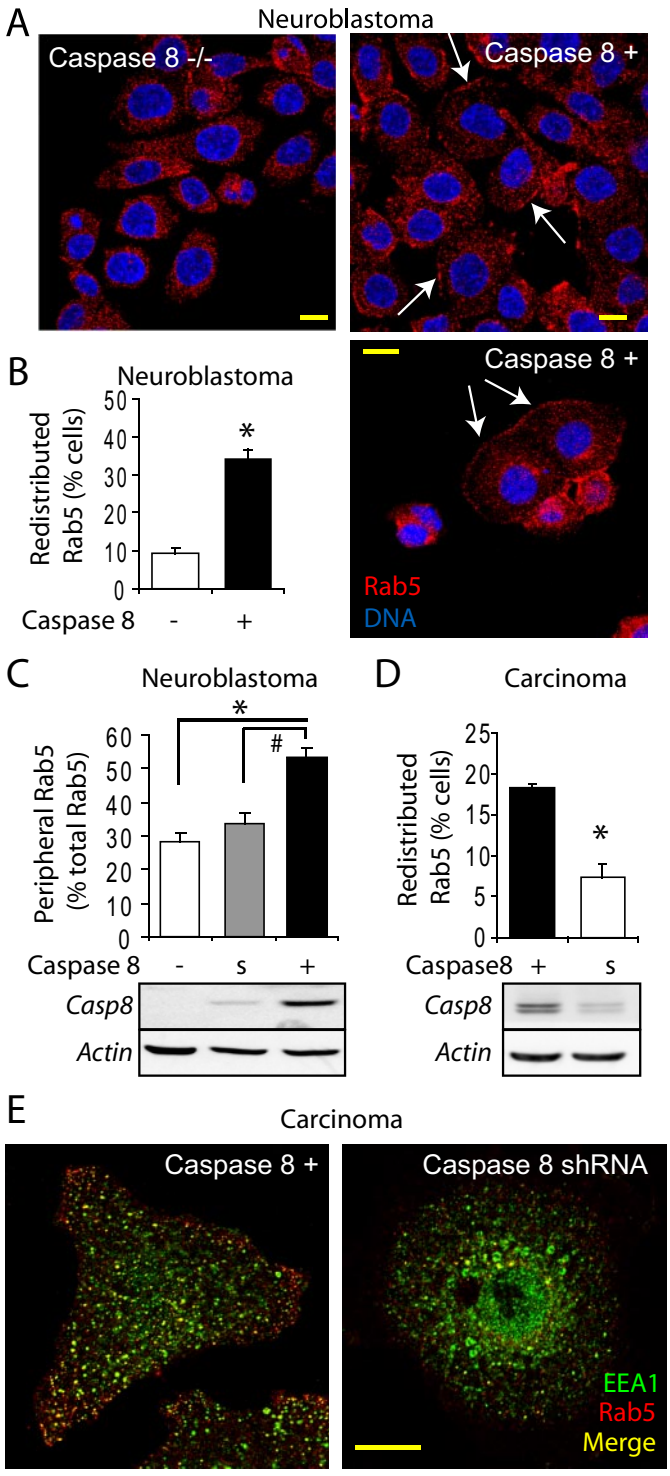

FIGURE 1. **Caspase 8 induces accumulation of Rab5 positive early endosomes at the cell periphery.** *A*, localization of Rab5 in neuroblastoma cells. NB7 neuroblastoma cells stably transfected with caspase 8 (NB7C8) were cultured for 24 h on glass coverslips and analyzed via confocal microscopy. Rab5 was detected with a mouse monoclonal antibody (*red channel*) and nuclei were stained with TOPRO-3 (DNA, *blue channel*). Representative pictures are shown for parental (*caspase 8 −/−*, *left panel*) and stably reconstituted cells (*caspase 8 +*, *right panel*). The *bar* represents 10 μm. *B*, incidence of cells exhibiting peripheral accumulation of Rab5. The percentage of cells with redistributed Rab5 was determined as described under "Experimental Procedures." Values obtained from each experiment were averaged from at least 10 pictures per sample (10–50 cells per field). Data shown represent the average of five independent experiments (mean ± S.E.). *, comparison with NB7 ($p < 0.001$). *C*, relative accumulation of Rab5 at the cell periphery. Neuroblastoma cells lacking (−), reconstituted for (+), or reconstituted and silenced (via short hairpin RNA (*shRNA*) for C8 (*s*)) expression of caspase 8 (see the *inset*) were analyzed by immunofluorescence, and the percentage of peripheral Rab5 was calculated relative to total Rab5 using the ImageJ software with the Radial Profile Plugin as described under "Experimental Procedures." *, $p < 0.01$; #, $p < 0.01$. *D*, A549 carcinoma cells subjected to lentiviral delivery of either empty vector (A549) or caspase 8 short hairpin RNA (A549/shC8) to suppress caspase 8 expression (*inset*, the *doublet band* corresponds to A and B isoforms) were analyzed by immunofluorescence as described above. The incidence of cells with peripheral accumulation of Rab5 was calculated as in *B*. Data are representative of three independent experiments, each one performed in triplicate (mean ± S.E.). *, $p < 0.001$. *E*, Rab5 was detected with a mouse monoclonal antibody (*red channel*), EEA1 was detected with a rabbit polyclonal antibody (*green channel*), and nuclei were stained with TO-PRO-3 (*blue channel*). The *bar* represents 10 μm. The peripheral accumulation of Rab5 (*red channel*) is evident.

8-deficient cells, with accumulation of Rab5 in the cell periphery (Fig. 1*A*). This altered distribution was selective to Rab5, with no changes in expression or distribution of EEA1, Rab7, and M6PR (data not shown), suggesting that at physiological levels of expression caspase 8 did not influence all aspects of the endocytic pathway. We were unable to determine whether overexpression of caspase 8 could further augment this effect or could induce changes to secondary endosomal pathways, as overexpression of caspase 8 induces apoptosis (data not shown).

In neuroblastoma cells lacking caspase 8, Rab5 was homogenously distributed throughout the cell body, with a minor accumulation at the cell periphery (Fig. 1, *A* and *B*). The accumulation of Rab5 at the cell periphery was dependent upon expression of caspase 8, as suppression of caspase 8 with short hairpin RNA ablated the accumulation of Rab5 in the periphery (Fig. 1*C*). To further evaluate the extent of Rab5 accumulated at the cell periphery, we measured the relative levels of Rab5 within the area located within a distance of 2–3 μm of peripheral edge of the cell (this distance represents ~25% of the cell; supplemental Fig. 1). As expected, a 2-fold increase of peripheral Rab5 was associated to expression of caspase 8 (Fig. 1*C*). These observations were confirmed in parallel studies expressing GFP-tagged caspase 8 in NB7 cells (supplemental Fig. 1). Overall co-localization of Rab5 with early (EEA1) or late endocytic proteins (Rab7, M6PR) was not generally affected by expression of caspase 8 (supplemental Fig. 2), confirming Rab5 as a specific target.

To extend these observations we also used A549 carcinoma cells in which endogenous caspase 8 was silenced (Fig. 1*D*). In agreement with the previous results, caspase 8 expression was associated with peripheral accumulation of Rab5, whereas loss of caspase 8 promoted a more homogenous distribution throughout the cell (Fig. 1*E*). The peripheral accumulation of Rab5 did not result from protein stabilization, as no significant differences in Rab5 protein levels were associated with caspase 8 expression (supplemental Fig. 3). Taken together, these data indicate that caspase 8 influences localization of Rab5 endosomes within the cell.

Importantly, most Rab5 (~95%) was found associated to membrane fractions, as revealed by subcellular fractionation (data not shown). These observations agree with previous reports (31). Only a slight variation in membrane-associated Rab5 was detected in caspase 8-expressing cells (93 or 97% total

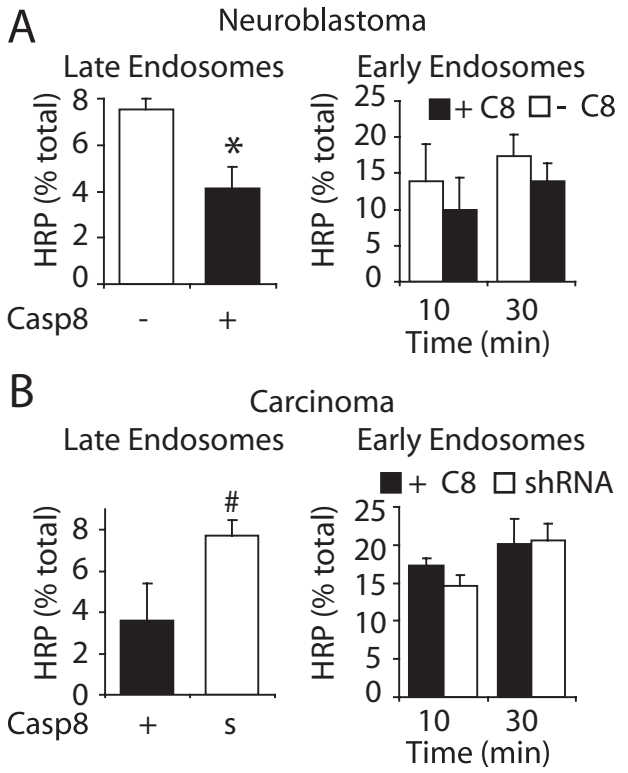

FIGURE 2. **Targeting of endocytosed HRP to late endosomes is decreased by caspase 8.** Internalization assays (37 °C by 30 min unless otherwise indicated) were performed to analyze the distribution of HRP within late and early endosome fractions. HRP activity was measured in each case and expressed as percentage of total activity. Data represent the average of three independent experiments (mean ± S.E.). *A*, neuroblastoma lacking caspase 8 (−) and stably reconstituted for caspase 8 (+); *, $p < 0.05$. *B*, carcinoma cells expressing caspase 8 (A549/control, +) or those with expression of caspase 8 suppressed (A549/shC8 (*s*)) were similarly compared; #, $p < 0.054$. *shRNA*, short hairpin RNA.

Rab5 was found associated to membranes in cells lacking or expressing caspase 8, respectively). Because most Rab5 is membrane-associated regardless the caspase 8 status, it would appear that relevant changes are in subcellular distribution of membrane-associated Rab5. The possibility that caspase 8 affects Rab5 shuttling between different early endosome populations or between early endosomes and the plasma membrane is unexpected and potentially important.

Caspase 8 Alters the Targeting of Cargo from Early to Late Endosomes—Because Rab5 is involved in trafficking of cargo from the plasma membrane to early and sorting endosomes (2), we evaluated whether caspase 8-mediated re-distribution of Rab5 influenced this process by tracking the accumulation of fluid-phase HRP in early and late endosomes. Analysis of purified endosome fractions (supplemental Fig. 4) revealed that the accumulation of HRP in late endosomes was substantially decreased in caspase 8-expressing neuroblastoma cells compared with caspase 8-deficient controls (Fig. 2*A*, *left panel*). Because substantial accumulation of HRP in late endosomes is observed only after 10–15 min of internalization (data not shown), we assayed late endosomes at 30 min internalization. Similar trends were obtained after 10 min of internalization, although variation was higher (Fig. 2*A* and data not shown). Conversely, no differences were observed in early endosomal HRP (Fig. 2*A*, *right panel*). Similarly, we observed an increased accumulation of HRP in late but not early endosomes from caspase 8-deficient carcinoma cells when compared with caspase 8-expressing control cells (Fig. 2*B*). The overall internalization rate was independent of caspase 8 expression in both carcinoma and neuroblastoma cells (data not shown and see below), implicating caspase 8 in regulating the delivery of cargo between the early and late endosome.

To test this possibility directly we tracked the internalization and localization of two differentially sorted cargos; that is, transferrin (*i.e.* cargo destined for recycling) and LDL (a cargo destined for degradation). We observed no difference in uptake of transferrin or LDL nor did we observe any changes in transferrin recycling as a function of caspase 8 expression (Fig. 3*A*). The distribution of internalized transferrin was similar in these cells and co-localized to the same degree with EEA1 and Rab5 regardless of caspase 8 expression (data not shown). By contrast, the intracellular distribution of internalized LDL was markedly different when caspase 8 was expressed. Among caspase 8-deficient cells, LDL was detected throughout the cell body (Fig. 3*B*, *upper left panel*), whereas in caspase 8-reconstituted cells a considerable retention of LDL was seen at the cell periphery, even 30 min of post-internalization (Fig. 3*B*, *upper right panel*). A partial co-localization of LDL with Rab5 was observed in caspase 8-expressing or -deficient cells, but this co-localization increased when caspase 8 was present (Fig. 3, *B* and *C*). These data demonstrated that expression of caspase 8 influenced the localization and fate of cargo destined to late endosomes. In fact, we observed the accumulation of LDL in Rab7-positive late endosomes (Fig. 4*A*) and M6PR-positive late endosomes and lysosomes (Fig. 4*B*) selectively among cells lacking caspase 8 (Fig. 4*C*). Importantly, caspase 8 did not affect expression or distribution of these protein markers for late endosomes (Fig. 4 and data not shown). Taken together, these results suggest that caspase 8 regulates the movement of cargo from early (Rab5) to late (Rab7) endosome compartments.

Caspase 8 Catalytic Activity Is Not Required to Influence Rab5 Localization—Proteolytic activity is required for the induction of apoptosis by caspase 8 but is dispensable for other activities, such as the promotion of cell migration (13, 14, 16). Both apoptosis and cell migration are dependent upon endocytic processes, and it was therefore unclear whether proteolytic activity was required for caspase 8 to regulate the Rab5-mediated trafficking. Therefore, we tested a neuroblastoma cell line stably reconstituted for a catalytically inactive mutant of caspase 8 (caspase 8/C360A). Interestingly, this mutant displayed an apparent accumulation of Rab5 at the cell periphery similar to cells expressing native caspase 8 (Fig. 5*A*). Moreover, the expression of catalytically inactive caspase 8 resulted in decreased accumulation of HRP tracer in late, but not early, endosomes (Fig. 5*B*). Thus, the mutant recapitulated the caspase 8 phenotype indicating that caspase 8 activity is not required for regulation of Rab5-mediated endosomal targeting.

Increased Rab5 GTP Loading in Cells Expressing Caspase 8—The processes of early endosome fusion, early-to-late endosome conversion, and subcellular localization depend on proper Rab5 activation/inactivation in time and space, which is governed by cycling between GTP binding and subsequent hydrolysis to GDP (for review, see Refs. 1 and 2). We assessed

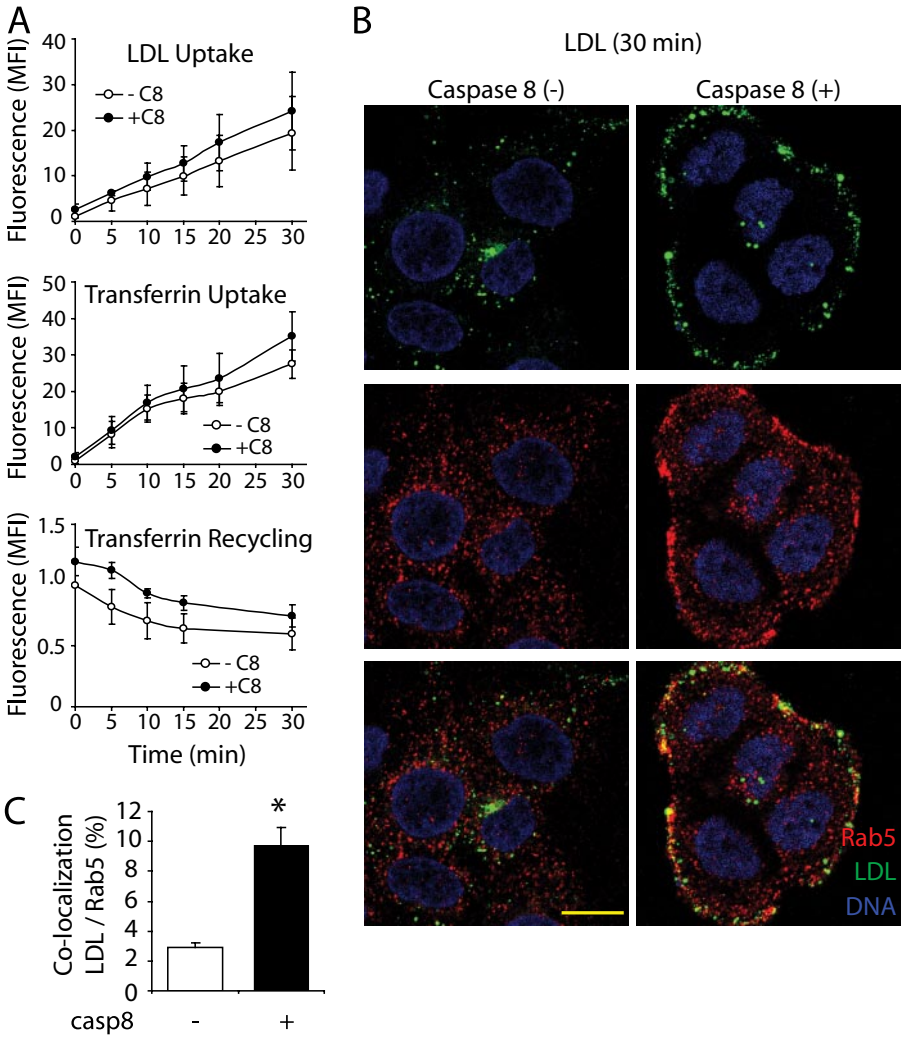

FIGURE 3. **LDL is retained at periphery of cells expressing caspase 8.** *A*, uptake of LDL or transferrin (*top* and *middle panels*) among neuroblastoma cells lacking caspase 8 (−*C8*) or stably reconstituted for caspase 8 (+*C8*) at times as indicated. Data were averaged from three independent experiments. Recycling of transferrin was also examined (*bottom panel*) as described. MFI, mean fluorescence intensity. *B*, the uptake of LDL (LDL-BODIPY-FL, *green channel*) was assessed after 15 min at 37 °C as described under "Experimental Procedures." Samples were analyzed via confocal microscopy, and Rab5 was detected with a mouse monoclonal antibody (*red channel*); DNA is counterstained with TO-PRO-3 (*blue channel*). Representative images are shown for neuroblastoma-deficient for caspase 8 (*caspase 8*−) or reconstituted for caspase 8 expression (*caspase 8*+). The *bar* represents 10 μm. *C*, analysis of the co-localization of Rab5 and LDL-BODIPY-FL. Analysis was performed by using the ImageJ software as indicated under "Experimental Procedures." Data represent the average of three independent experiments (mean ± S.E.). *, $p < 0.001$.

whether caspase 8 influenced Rab5 GTP loading using a pull-down approach with a fusion protein that selectively binds GTP-loaded Rab5 (GST-R5BD) (32). The system selectively bound "constitutively active" Rab5 mutant Rab5/Q79L (GTPase-deficient) but not the GDP binding "dominant negative" Rab5/S34N (26) mutant (Fig. 6*A*, *left panel*). Importantly, we detected increased levels of GTP-bound Rab5 among cells expressing caspase 8 relative to cells lacking caspase 8 (Fig. 6*A*, *right panel*). Densitometry confirmed that GTP loading of endogenous Rab5 was significantly (~2.5-fold) increased in caspase 8-expressing cells (Fig. 6*B*). Similar results were seen in transient transfection systems (supplemental Fig. 5), leading us to conclude that caspase 8 expression influences Rab5 activity as well as localization.

Rab5 Activity Is Regulated by Caspase 8 via p85α—We next sought to evaluate the molecular mechanism by which caspase 8 could influence Rab5 GTP loading and function. Interestingly, the SH2 domains of p85α were recently shown to interact with a phosphorylated tyrosine (Tyr-380) located in a peptide loop between the small and large subunits of the catalytic domain of caspase 8. Interactions between SH2 domains and this tyrosine do not require caspase 8 catalytic activity (13, 16). Moreover, p85α acts as a Rab-GAP, promoting Rab5 hydrolysis of GTP (8). Therefore, we sought to determine whether p85α was a critical intermediate in the caspase 8-regulated Rab5 function.

We first evaluated whether caspase 8 and p85α interacted within our cells. Indeed, p85α co-precipitated with caspase 8 from cells stably (Fig. 6*C*) or transiently (supplemental Fig. 5) expressing caspase 8. Next, we tested whether the expression of p85α influenced Rab5 loading. As shown for endogenous Rab5 (Fig. 6*B*), caspase 8 induced an ~8-fold increase in GTP loading of an exogenous Rab5 reporter (Fig. 6*D*). Importantly, p85α expression overcame the capacity of caspase 8 to promote Rab5 GTP loading (Fig. 6*D* and supplemental Fig. 5). Therefore, we sought to evaluate whether caspase 8 and p85α act reciprocally to control Rab5 activity. To test this possibility we used GFP-tagged caspase 8 mutants which were catalytically inactive (C360A) or unable to interact with p85α (Y380F) (16). Neuroblastoma cells stably transfected with these mutants confirmed that catalytic activity was not required for promotion of Rab5 GTP loading (Fig. 7*A*). However, mutation of the SH2 binding site that disrupted p85α association (Y380F) abrogated the ability of caspase 8 to increase Rab5 GTP loading (Fig. 7, *A*–*C*). The findings were extended using HEK293T cells transiently transfected with either GFP alone (control) or GFP-tagged caspase 8, caspase 8/C360A, or caspase 8/Y380F. As in the neuroblastoma cells, expression of both wild type caspase 8-GFP or caspase 8/C360A-GFP, but not caspase 8/Y380F-GFP, increased Rab5-GTP levels (supplemental Fig. 6). These data raised the notion that p85α association with caspase 8 might influence its ability to bind Rab5 and thereby promote GTP hydrolysis.

To address this, we expressed a p85α/R274A mutant (GAP-deficient) and a p85α/R368A/R649A double mutant (termed ΔR) which lacked SH2-tyrosine binding activity (8) in neuroblastoma

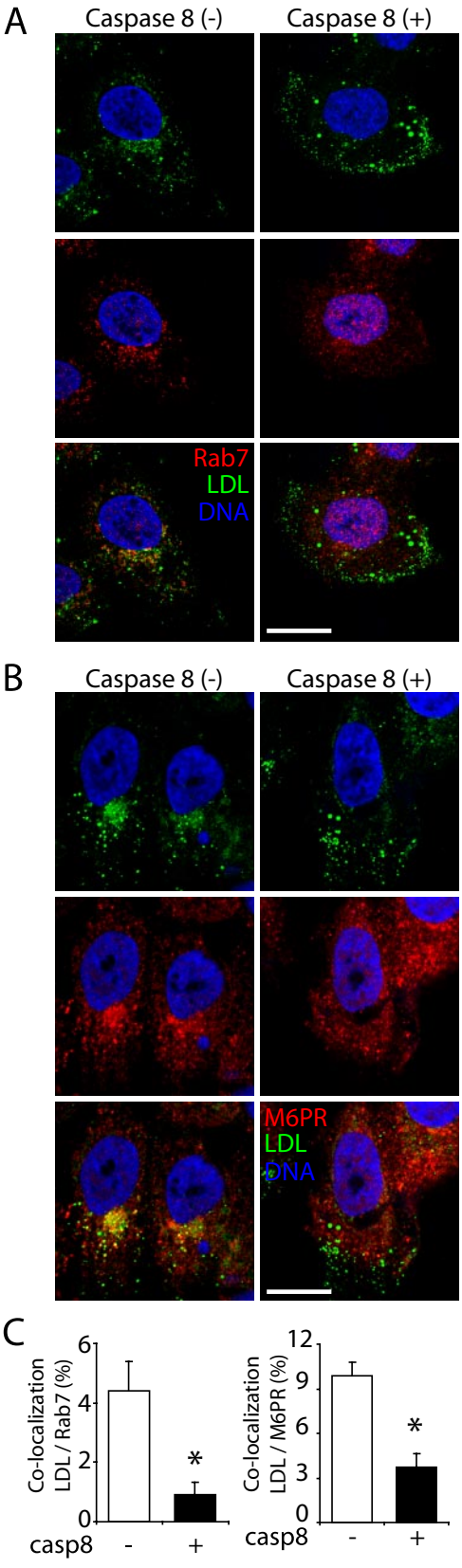

FIGURE 4. **Caspase 8 decreases delivery of endocytosed LDL to late endosomes.** *A* and *B*, uptake of LDL (*green channel*) was performed and assessed with respect to delivery to late endosomes. Late endosome were identified by antibodies to Rab7 (*A*) and M6PR (*B*) as indicated (*green channels*), and DNA was counterstained with TO-PRO-3 (*blue channel*). Representative images are shown for cells deficient in caspase 8 (*caspase 8*−) or reconstituted for caspase 8 (*caspase 8*+). The *bar* represents 10 μm. *C*, colocalization analysis of Rab7 or M6PR and LDL-BODIPY-FL. Analysis was performed by using the ImageJ software as described above. Data represent the average of three independent experiments (mean ± S.E.). *, in both cases $p < 0.05$.

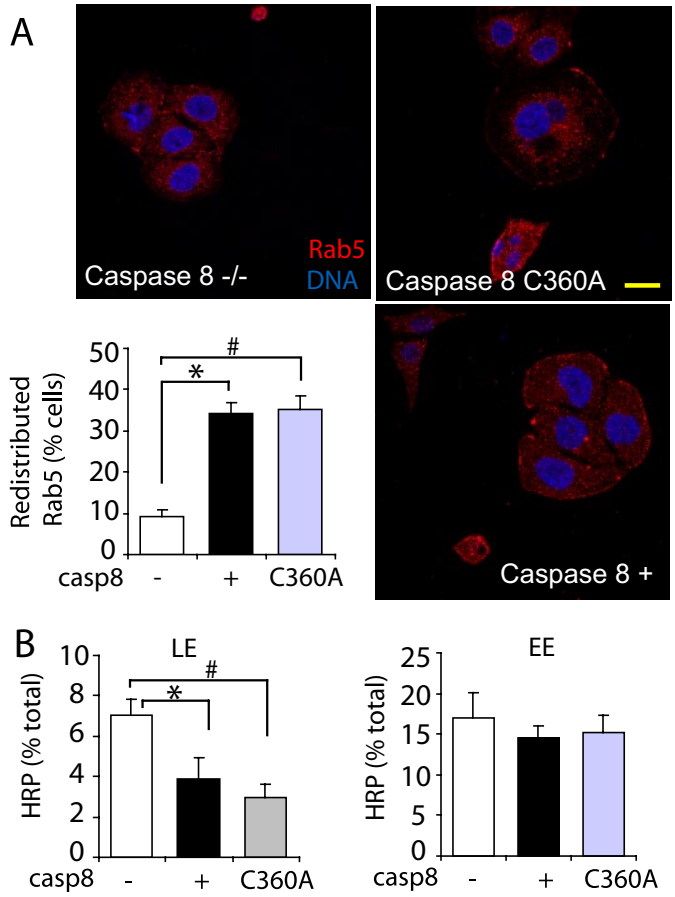

FIGURE 5. **Proteolytic activity of caspase 8 is not required for altered Rab5 localization and late endosome targeting of cargo.** *A*, neuroblastoma cells deficient for caspase 8 (*caspase 8* −/−) or stably reconstituted for active (*caspase 8*+) or inactive caspase 8 expression (*caspase 8 C360A*) were analyzed for Rab5 localization. Rab5 was detected with a mouse monoclonal antibody (*red channel*) and DNA stained with TO-PRO-3 (*blue channel*). The *bar* represents 10 μm. The incidence of cells with peripheral accumulation of Rab5 was calculated as described in Fig. 1*B*. The result is representative of three independent experiments (mean ± S.E.). *, $p < 0.001$; #, $p < 0.001$. *B*, HRP accumulation in cells deficient for caspase 8 (*caspase 8* −/−) or stably reconstituted for active (*caspase 8*+) or inactive caspase 8 (*caspase 8 C360A*) was analyzed as described above. Data were averaged from three independent experiments (mean ± S.E.). *, $p < 0.05$; #, $p < 0.05$. LE, late endosome; EE, early endosome.

cells expressing caspase 8. Rab5 GTP loading was then measured. Although expression of wild type p85α suppressed Rab GTP loading, this required Rab5-GAP activity, as the p85α/R274A mutant could not overcome the caspase 8-mediated effect. Similarly, phosphotyrosine binding activity of p85α was critical to overcoming caspase 8-induced GTP loading, as loss of caspase 8 binding in the p85α/ΔR mutants permitted caspase 8-induced Rab5 GTP loading (Fig. 7*D*). Based on these results, we propose a simple initial model wherein caspase 8 may increase Rab5 GTP loading by interfering with Rab5 GAP activity of p85α via SH2 interactions with Tyr-380 of caspase 8 (Fig. 8).

The role of p85α in caspase 8-mediated regulation of Rab5 was reflected in the localization of this protein. Expression of

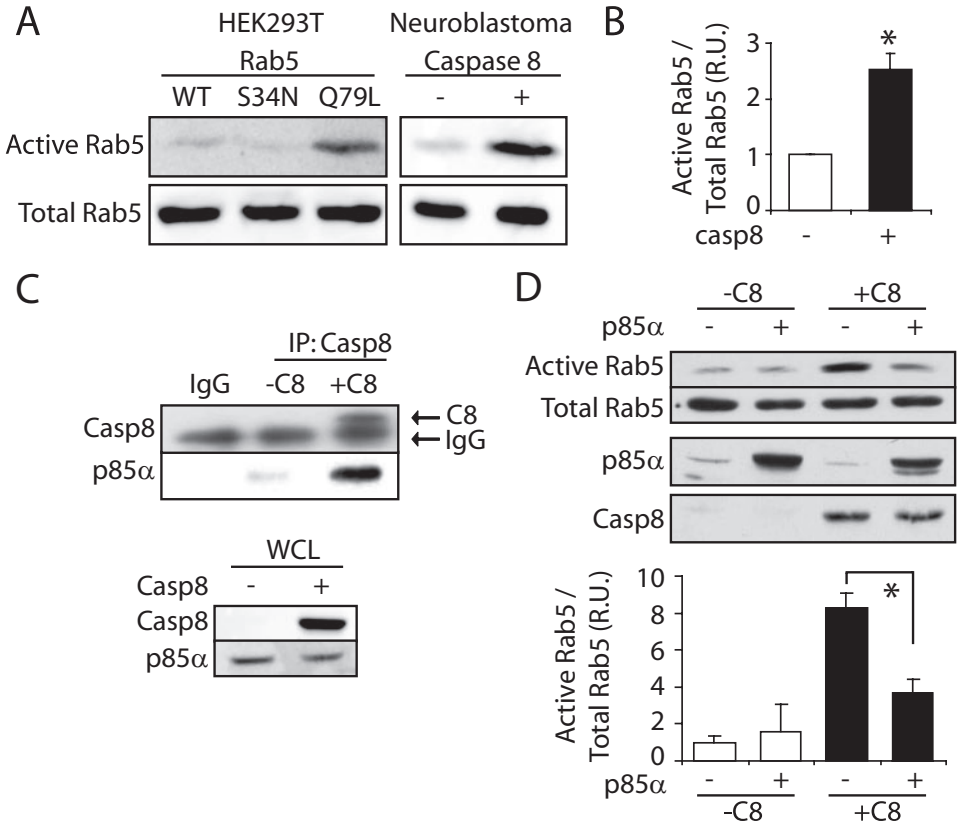

FIGURE 6. **Caspase 8 increases Rab5 GTP loading.** *A*, Rab5-GTP levels were assessed using a GST-R5BD pulldown assay as described under "Experimental Procedures." *Left panel*, HEK293T cells were transiently transfected with wild type (*WT*) Rab5, Rab5/S34N, or Rab/Q79L mutants. After 24 h cells were lysed, and GTP-loaded Rab5 was pulled down with GST-R5BD. *Right panel*, neuroblastoma cells lacking or expressing caspase 8 were subjected to similar analysis. *B*, Rab5-GTP levels were normalized to total input Rab5 and quantified by scanning densitometry of three independent experiments (mean ± S.E.). *, $p < 0.01$. *RU*, relative units. *C*, caspase 8 immunoprecipitated (*IP*) from confluent cultures of neuroblastoma cells was assessed for the presence of associated p85α as detected by immunoblotting. *WCL*, whole cell lysates. *D*, Rab-GTP levels were measured as in *A*, among neuroblastoma cells ectopically expressing Rab5. NB7 lacking or expressing caspase 8 were either co-transfected with Rab5 and empty vector or Rab5 and p85α. Cell lysates were generated 24 h post-transfection, and Rab5-GTP levels were measured. *Upper panel*, a representative Western blotting from three independent experiments is shown; the *lower graph* shows an average from three independent experiments by scanning densitometry (mean ± S.E.). *, $p < 0.005$.

wild type, but not p85α/R274A or p85α/ΔR, prevented the accumulation of peripheral Rab5 in caspase 8-expressing cells (supplemental Fig. 7*A*, *lower panels*). Conversely, expression of the Rab-GAP deficient p85α allows the accumulation of Rab5 in the periphery of caspase 8-negative cells (supplemental Fig. 7*A*, *upper panels*). Finally, unlike wild type (Fig. 1) or catalytically deficient caspase 8 (Fig. 5), caspase 8/Y380F did not induce accumulation of Rab5 at the cell periphery (supplemental Fig. 7*B*), further supporting the requirement of p85α binding for this regulation.

DISCUSSION

Caspase 8 has been associated with endocytic vesicles during execution of the apoptotic pathway (10–12) and has been implicated in endosome remodeling after a pro-apoptotic stimuli during the type II extrinsic pathway (33). In these cases apoptosis is dependent upon caspase 8 activity. Here, we report a novel role for caspase 8 in controlling Rab5 localization, activity, and function. The presence of caspase 8 in a variety of cells was shown to modify early endosome topology; in particular, the accumulation of Rab5-positive endosomes at the cell periphery. In agreement with this we observed concurrent changes in cargo transport from early to late endosomes and found that these events were associated with caspase 8-dependent increases in the levels of GTP-bound Rab5.

Our results are somewhat surprising with respect to previous reports using overexpression strategies to map Rab5 activity (34). We did not observe formation of enlarged early endosomes by caspase 8 (despite the fact that caspase 8 increased GTP loading of Rab5). Compared with the previously reported enlargement of early endosomes by expression of the Rab/Q79L mutant (26), the caspase 8 impact on Rab5 function was less pronounced. We could duplicate the prior reported effects by expression of Rab5/Q79L, but not Rab5/S34N, which led to formation of enlarged early endosomes in our cells. This approach revealed a substantial increase in co-localization of Rab5 with EEA1 (data not shown). Although informative, the concern with any overexpression system is that some of the effects observed may be exaggerated relative to a cell's normal physiology. Indeed, we observed no increase of EEA1/Rab5 colocalization among cells expressing caspase 8 (supplemental Fig. 2). Alternatively, such differences in localization may reflect the observation that caspase 8 also activates the small GTPase Rac (15). Thus, it remains possible that coordinate Rac and Rab5 activation results in peripheral retention of early endosomes, which might not be observed after simple expression of active Rab5. Nonetheless, our data are consistent with a model proposing a dynamic and reversible assembly of Rab5 domains in early endosomes with a cycling-dependent "handoff" to Rab7 (35, 36).

In contrast to the role of caspase 8 during apoptosis, no proteolytic activity was required to modify endosomal targeting. These data differ from caspase-3, a related enzyme that has been reported to alter transport via a proteolysis-dependent mechanism (37). Nonetheless, recent evidence supports non-apoptotic functions for caspase 8 that are independent of catalytic activity, with several studies supporting a role for caspase 8 in cell migration and invasion (13–16, 22). In fact, caspase 8 was found to be phosphorylated on tyrosine 380 in these studies. This event compromises caspase 8 activation (13).

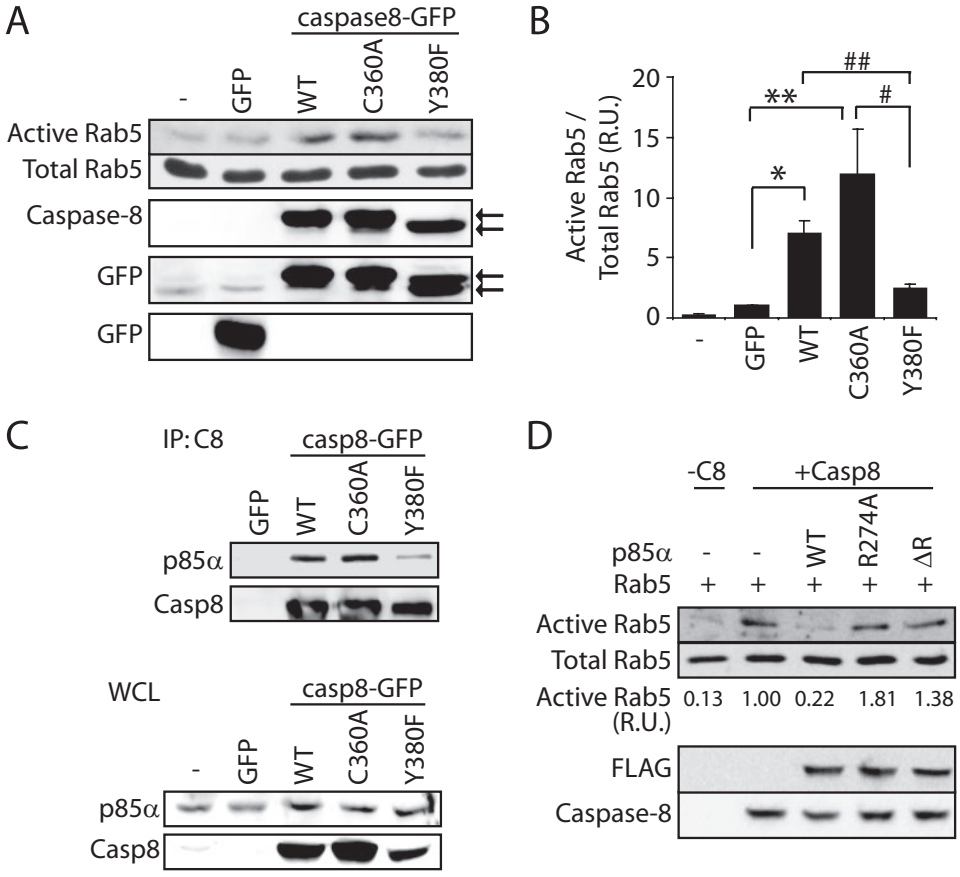

FIGURE 7. **Molecular requirements for caspase 8-mediated Rab5 GTP loading.** *A*, Rab5 GTP loading was assessed by using the GST-R5BD pulldown assay among neuroblastoma cells expressing active caspase 8, inactive caspase 8(C360A), or a caspase 8 mutant deficient for phosphorylation at the Tyr-380 SH2 binding site. Extracts were obtained from 24-h growth cultures, and Rab5-GTP levels were measured. *Arrows* indicate the relative mass of caspase 8 or the nonphosphorylatable caspase 8 mutant. A representative Western blotting from three independent experiments is shown. *WT*, wild type. *B*, data were evaluated from three independent experiments by scanning densitometry (mean ± S.E.). *, $p < 0.005$; **, $p < 0.05$; #, $p < 0.05$; ##, $p < 0.1$. *RU*, relative units. *C*, caspase 8 was immunoprecipitated (*IP*) from confluent cultures of expressing GFP-tagged caspase 8 constructs. Caspase 8 and p85α were detected by Western blotting in immunoprecipitates (*upper panel*) and 25 μg of whole cell lysates (*WCL*, *lower panel*). *D*, neuroblastoma cells expressing caspase 8 were co-transfected with either Rab5 or pcDNA3.1 (empty vector control) or with Rab5 and FLAG-tagged "wild type" p85α, Rab-GAP deficient p85 (p85α/R274A), or SH2-inactive p85 (p85α/R368A/R649A (Δ*R*). After 24 h, Rab5-GTP levels were measured. Rab5 (*upper panel*), FLAG, and caspase 8 (*lower panel*) were detected by Western blotting. *Numbers* indicate Rab5-GTP levels normalized to total Rab5 by densitometry averaged from two independent experiments.

It is not yet clear whether caspase 8 phosphorylation blocks caspase catalytic activity directly; however, it does create an SH2 binding site bound by Src family kinases (13) and by the SH2 domains of p85α (16). This SH2 binding site has been shown to be critical for recruitment of caspase 8 to the cell periphery (13). Thus, caspase 8 maturation and proteolytic activity could be regulated conformationally or via sequestration after SH2 binding. In this case we observe a robust association with p85α, a known Rab-GAP, and caspase 8, which is abrogated in a non-phosphorylated Y380F mutant. The adaptor protein p85α is a known regulator of endocytosis that can act through a number of mechanisms. Here we show that increased expression of p85α overcomes the effect of caspase 8 expression, decreasing Rab5 GTP loading; however, this requires both p85α Rab-GAP activity and SH2 binding function. Together the results suggest a model in which caspase 8 is located proximal to p85α and binds to it in a manner that influences its ability to regulate Rab5 (Fig. 8).

It is clear that alterations in endocytosis can affect a number of different cell pathways. In particular, cell migration and delivery of cell surface receptors are directly controlled by mechanisms involving Rab5 activation and re-localization (23). Our observation that caspase 8 influences endosome dynamics may provide mechanistic insights into how this protease regulates cell motility (13, 16). The recently reported role of Rab5 in guiding Rac signaling has clear implications for cell migration (23). An intricate relationship between Rab5 and the integrin trafficking (18, 38) suggests coordinated signaling among endocytic, cytoskeletal, and apoptotic pathway during cell migration. These results provide a new basis to begin to understand the molecular mechanisms by which caspase 8 impacts tumor cell biology.

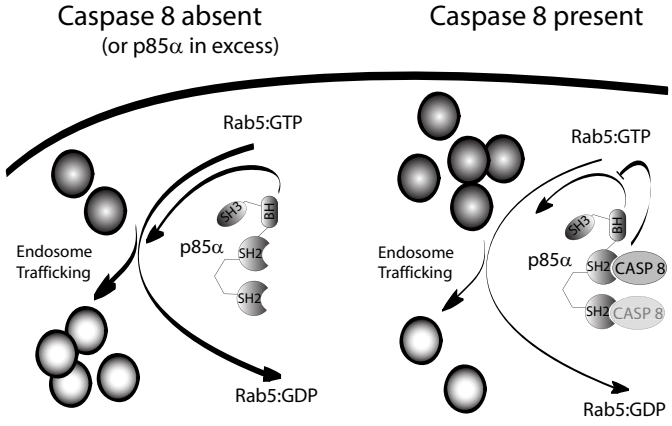

FIGURE 8. **Model showing the role of caspase 8 in regulating Rab5 activity.** A simple mechanism by which caspase 8 expression may influence Rab5-GTP levels and endosomal maturation via its ability to bind to p85α is shown.

Acknowledgments—We thank Drs. Guy Salvesen, Sandra Schmidt, and Jill Lahti for the gift of reagents.

REFERENCES

1. Markgraf, D. F., Peplowska, K., and Ungermann, C. (2007) *FEBS Lett.* **581,** 2125–2130
2. Zerial, M., and McBride, H. (2001) *Nat. Rev. Mol. Cell Biol.* **2,** 107–117
3. Simonsen, A., Lippe, R., Christoforidis, S., Gaullier, J. M., Brech, A., Cal-

laghan, J., Toh, B. H., Murphy, C., Zerial, M., and Stenmark, H. (1998) *Nature* **394,** 494–498
4. Stenmark, H., Vitale, G., Ullrich, O., and Zerial, M. (1995) *Cell* **83,** 423–432
5. Nielsen, E., Christoforidis, S., Uttenweiler-Joseph, S., Miaczynska, M., Dewitte, F., Wilm, M., Hoflack, B., and Zerial, M. (2000) *J. Cell Biol.* **151,** 601–612
6. Christoforidis, S., Miaczynska, M., Ashman, K., Wilm, M., Zhao, L., Yip, S. C., Waterfield, M. D., Backer, J. M., and Zerial, M. (1999) *Nat. Cell Biol.* **1,** 249–252
7. Lawe, D. C., Patki, V., Heller-Harrison, R., Lambright, D., and Corvera, S. (2000) *J. Biol. Chem.* **275,** 3699–3705
8. Chamberlain, M. D., Berry, T. R., Pastor, M. C., and Anderson, D. H. (2004) *J. Biol. Chem.* **279,** 48607–48614
9. Chamberlain, M. D., Chan, T., Oberg, J. C., Hawrysh, A. D., James, K. M., Saxena, A., Xiang, J., and Anderson, D. H. (2008) *J. Biol. Chem.* **283,** 15861–15868
10. Algeciras-Schimnich, A., Shen, L., Barnhart, B. C., Murmann, A. E., Burkhardt, J. K., and Peter, M. E. (2002) *Mol. Cell. Biol.* **22,** 207–220
11. Lee, K. H., Feig, C., Tchikov, V., Schickel, R., Hallas, C., Schutze, S., Peter, M. E., and Chan, A. C. (2006) *EMBO J.* **25,** 1009–1023
12. Schneider-Brachert, W., Tchikov, V., Neumeyer, J., Jakob, M., Winoto-Morbach, S., Held-Feindt, J., Heinrich, M., Merkel, O., Ehrenschwender, M., Adam, D., Mentlein, R., Kabelitz, D., and Schutze, S. (2004) *Immunity* **21,** 415–428
13. Barbero, S., Barila, D., Mielgo, A., Stagni, V., Clair, K., and Stupack, D. (2008) *J. Biol. Chem.* **283,** 13031–13034
14. Finlay, D., and Vuori, K. (2007) *Cancer Res.* **67,** 11704–11711
15. Helfer, B., Boswell, B. C., Finlay, D., Cipres, A., Vuori, K., Bong Kang, T., Wallach, D., Dorfleutner, A., Lahti, J. M., Flynn, D. C., and Frisch, S. M. (2006) *Cancer Res.* **66,** 4273–4278
16. Senft, J., Helfer, B., and Frisch, S. M. (2007) *Cancer Res.* **67,** 11505–11509
17. Barnhart, B. C., Legembre, P., Pietras, E., Bubici, C., Franzoso, G., and Peter, M. E. (2004) *EMBO J.* **23,** 3175–3185
18. Pellinen, T., and Ivaska, J. (2006) *J. Cell Sci.* **119,** 3723–3731
19. Stupack, D. G., Teitz, T., Potter, M. D., Mikolon, D., Houghton, P. J., Kidd, V. J., Lahti, J. M., and Cheresh, D. A. (2006) *Nature* **439,** 95–99
20. Teitz, T., Wei, T., Valentine, M. B., Vanin, E. F., Grenet, J., Valentine, V. A., Behm, F. G., Look, A. T., Lahti, J. M., and Kidd, V. J. (2000) *Nat. Med.* **6,** 529–535
21. Cursi, S., Rufini, A., Stagni, V., Condo, I., Matafora, V., Bachi, A., Bonifazi, A. P., Coppola, L., Superti-Furga, G., Testi, R., and Barila, D. (2006) *EMBO J.* **25,** 1895–1905
22. Frisch, S. M. (2008) *Cancer Res.* **68,** 4491–4493
23. Palamidessi, A., Frittoli, E., Garre, M., Faretta, M., Mione, M., Testa, I., Diaspro, A., Lanzetti, L., Scita, G., and Di Fiore, P. P. (2008) *Cell* **134,** 135–147
24. Spaargaren, M., and Bos, J. L. (1999) *Mol. Biol. Cell* **10,** 3239–3250
25. Wrasidlo, W., Mielgo, A., Torres, V. A., Barbero, S., Stoletov, K., Suyama, T. L., Klemke, R. L., Gerwick, W. H., Carson, D. A., and Stupack, D. G. (2008) *Proc. Natl. Acad. Sci. U. S. A.* **105,** 2313–2318
26. Stenmark, H., Parton, R. G., Steele-Mortimer, O., Lutcke, A., Gruenberg, J., and Zerial, M. (1994) *EMBO J.* **13,** 1287–1296
27. Brown, T. C., Tran, I. C., Backos, D. S., and Esteban, J. A. (2005) *Neuron* **45,** 81–94
28. Liu, J., Lamb, D., Chou, M. M., Liu, Y. J., and Li, G. (2007) *Mol. Biol. Cell* **18,** 1375–1384
29. Gorvel, J. P., Chavrier, P., Zerial, M., and Gruenberg, J. (1991) *Cell* **64,** 915–925
30. Gu, F., Aniento, F., Parton, R. G., and Gruenberg, J. (1997) *J. Cell Biol.* **139,** 1183–1195
31. Chavrier, P., Parton, R. G., Hauri, H. P., Simons, K., and Zerial, M. (1990) *Cell* **62,** 317–329
32. Vitale, G., Rybin, V., Christoforidis, S., Thornqvist, P., McCaffrey, M., Stenmark, H., and Zerial, M. (1998) *EMBO J.* **17,** 1941–1951
33. Reinehr, R., Sommerfeld, A., Keitel, V., Grether-Beck, S., and Haussinger, D. (2008) *J. Biol. Chem.* **283,** 2211–2222
34. Galperin, E., and Sorkin, A. (2003) *J. Cell Sci.* **116,** 4799–4810
35. Del Conte-Zerial, P., Brusch, L., Rink, J. C., Collinet, C., Kalaidzidis, Y., Zerial, M., and Deutsch, A. (2008) *Mol. Syst. Biol.* **4,** 206–214
36. Rink, J., Ghigo, E., Kalaidzidis, Y., and Zerial, M. (2005) *Cell* **122,** 735–749
37. Santambrogio, L., Potolicchio, I., Fessler, S. P., Wong, S. H., Raposo, G., and Strominger, J. L. (2005) *Nat. Immunol.* **6,** 1020–1028
38. Pellinen, T., Arjonen, A., Vuoriluoto, K., Kallio, K., Fransen, J. A., and Ivaska, J. (2006) *J. Cell Biol.* **173,** 767–780